Research In Microbiology
December 2009, Volume 160 Issue 10 Pages 838-847
https://doi.org/10.1016/j.resmic.2009.09.017
https://archimer.ifremer.fr/doc/00815/92746/

Proteomic investigation of enzymes involved in 2-ethylhexyl nitrate biodegradation in *Mycobacterium austroafricanum* IFP 2173

Nicolau Elodie [1, 3, 4], Kuhn Lauriane [2], Marchal Remy [4], Jouanneau Yves [1, 3, *]

[1] Laboratoire de Chimie et Biologie des Métaux, CEA, iRTSV, 17, rue des Martyrs, 38054 Grenoble, France
[2] Laboratoire d'Etude de la Dynamique des Protéomes, CEA, iRTSV, 38054 Grenoble, France
[3] CNRS-UMR5249, 38054 Grenoble, France
[4] Département de Biotechnologie, Institut Français du Pétrole, 92852 Rueil-Malmaison Cedex, France

Corresponding author : Yves Jouanneau, email address : yves.jouanneau@cea.fr

nicolau.elodie@gmail.com ; lauriane.kuhn@pansanel.net ; remy.marchal@ifp.fr

Abstract :

2-Ethyhexyl nitrate (2-EHN) is a synthetic chemical used as a diesel fuel additive, which is recalcitrant to biodegradation. In this study, the enzymes involved in 2-EHN degradation were investigated in Mycobacterium austroafricanum IFP 2173. Using two-dimensional gel electrophoresis and a shotgun proteomic approach, a total of 398 proteins appeared to be more abundant in cells exposed to 2-EHN than in acetate-grown cells. This set of proteins includes multiple isoenzymes of the beta-oxidation pathway, two alcohol and one aldehyde dehydrogenase, as well as four cytochromes P450, including one CYP153 which functions as an alkane hydroxylase. Strain IFP 2173 was also found to contain two alkB-like genes encoding putative membrane-bound alkane hydroxylases. RT-PCR experiments showed that the gene encoding the CYP153 protein, as well as alkB genes, were expressed on 2-EHN. These findings are discussed in the light of a recently proposed 2-EHN degradation pathway involving an initial attack by an alkane hydroxylase and one turn of beta-oxidation, leading to the accumulation of a gamma-lactone as a deadend product.

Keywords : Alkane hydroxylase, Cytochrome P450, CYP153, 2-Ethylhexyl nitrate, Mycobacterium austroafricanum, beta-oxidation

Abbreviations : ADH : alcohol dehydrogenase ; ALDH : aldehyde dehydrogenase ; 2-EHN : 2-ethylhexyl nitrate ; SDR : short-chain dehydrogenase/reductase

1. **Introduction**

2-Ethylhexyl nitrate (2-EHN) is a xenobiotic compound used as a gasoline additive. Due to its explosive properties, 2-EHN is considered as the best cetane improver for diesel oil, including bio-diesels that might be used in the near future [1; 25]. In case of accidental release, 2-EHN is a serious health hazard, as humans exposed to this chemical were found to suffer from various symptoms, including headache, dizziness, chest discomfort, palpitations or nausea [7]. Although 2-EHN was considered not readily biodegradable by US EPA [26]), it was recently reported that it could be degraded by *Mycobacterium austroafricanum* [24].

Soil *Mycobacteria* have been described for their ability to degrade a wide range of aliphatic and aromatic hydrocarbons, including polycyclic aromatic hydrocarbons [3; 10; 33], and fuel additives such as methyl *tertio*-butyl-ether [5; 13]. These bacteria are well equipped to degrade hydrocarbons, which they used as carbon sources. Their bacterial wall, rich in mycolic acids, confers resistance to toxic hydrophobic pollutants and, on the other hand, may facilitate access to hydrocarbons [12; 22]. Moreover, soil *Mycobacteria* contain oxygenases of different types, which play a crucial role in the degradation of both aliphatic and aromatic hydrocarbons. For instance, monooxygenases catalyze the first step in the degradation of alkanes. C_5-C_{16} alkanes are substrates of two kinds of enzymes, either integral-membrane non-heme diiron monooxygenases (AlkB) [29], or cytochromes P450 [14]. Growth on alkanes requires metabolic adaptation, as shown through a proteomic analysis of the marine bacterium *Alcanivorax borkumensis* SK2 [18]. This study revealed that alkane utilisation may proceed via different pathways, involving two AlkB hydroxylases, one putative flavin monooxygenase, and three P450 cytochromes. Moreover, bacterial adaptation to alkane utilisation resulted in a strongly modified metabolism, with consequences for carbon flow and membrane lipid composition [18]. In recent years, high-throughput proteomics was implemented to identify whole sets of enzymes involved in complex bacterial metabolic pathways, such as the biodegradation of aromatic hydrocarbons [9].

Combined with functional genomics, proteomics helps understand cell response to environmental stimuli and may prove useful to develop efficient bioremediation strategies [34].

In previous studies, *M. austroafricanum* IFP 2173 was isolated on iso-octane [23], then selected for its ability to degrade 2-EHN [24]. Degradation of 2-EHN was found to be incomplete, yielding a 6-carbon γ-lactone, which accumulated as a dead-end product. A degradation pathway was proposed involving hydroxylation of the methyl group in distal position, then oxidation to the carboxylic acid, and further metabolism through one cycle of β-oxidation [17]. In order to identify the enzymes involved in this pathway, we have undertaken a proteomic analysis of cells exposed to 2-EHN. Because the genome sequence of strain IFP 2173 is unknown, we tentatively identified relevant proteins by comparing their peptide sequences to those of orthologs found in the data bases. Currently, 21 genome sequences of *Mycobacterium* strains are available, six of which are from fast-growing strains isolated from soil, and genome annotation of *M. smegmatis* and related species has been assessed by proteomic analysis [6]. Besides focusing on enzymes involved in 2-EHN degradation, this study gives an insight into proteins possibly involved in the response of bacteria to exposure to a toxic and hydrophobic xenobiotic compound.

2. Material and Methods

2.1 Bacterial strain and growth conditions

M. austroafricanum strain IFP 2173 was grown on a mineral salts medium at 30°C as described previously [17]. The carbon source was sodium acetate (4 g/l) or 2-EHN (500 mg/l). Growth was monitored by measurements of the optical density (OD) at 600 nm. To prepare 2-EHN-induced cells, acetate-grown cells were washed and resuspended to an OD_{600} of 1.5 in culture medium, then incubated for five days with 2-EHN in conical flasks sealed with Teflon-coated screw caps.

2.2 In vivo ^{35}S labelling of proteins

For labelling experiments, bacteria were incubated with 2-EHN or acetate (control) in the presence of a mixture of ^{35}S-labelled methionine and cysteine (0.1 mCi, Easytag Express protein-labelling mix; NEN Life Science Products). Bacteria were incubated for 6 h on acetate or 30 h on 2-EHN at 30°C. In a control experiment, bacteria were incubated without exogenous C-source for 30h. Protein extracts were prepared as described below and analyzed by 2D electrophoresis and SDS-PAGE.

2.3 Preparation of protein extracts

Cell-free extracts were prepared by ultrasonication as described previously [10]. Ultracentrifugation at 240,000 × *g* for 1 h was performed to separate soluble proteins from the membrane fraction, using an Optima TLX Ultracentrifuge (Beckman Instruments). Supernatant fractions were treated with benzonase (2,000 U; Merck), and subsequently dialysed for 4-5 h at 4°C against 5 mM phosphate buffer, pH 7.5, containing 1 mM $MgCl_2$, then overnight against ultrapure water. Samples were immediately processed as described below or stored at -20°C.

2.4 Two dimensional gel electrophoresis

Two-dimensional (2D) gel electrophoresis was carried out as described previously [10], with minor modifications. Briefly, 400 µg protein samples (or labelled extracts equivalent to 4.2 10^4 cpm) were applied to 18-cm IPG strips (ReadyStrip; Biorad) and fractionated in the pH range 4 to 7 by isoelectric focusing for a total of approximately 70 kVh. Second dimension electrophoresis was carried out on 12.5 % polyacrylamide gels in a Protean II xi cell (Biorad) at 20 mA per gel for 15-16 h, using a Tris-glycine buffer system [11]. The proteins were visualised by colloidal blue G-250 staining as described by Neuhoff [16], except that ethanol replaced methanol. ^{35}S labelled gels were stained, dried, and exposed to X-ray films for 3 weeks (Kodak BioMax MR). All gels were performed in triplicate, except for gels containing labelled proteins. Comparison of 2D gel patterns and spot intensities was carried out by visual inspection of gels.

Only spots that were absent in control extracts or that repeatedly showed an estimated intensity at least twice as high on 2-EHN extracts compared to control extracts were taken into consideration. Protein spots of interest were excised from the gel and processed for in-gel protein digestion and LC-MS/MS analysis as described below. Proteins up-regulated in acetate-grown cells are not discussed in this study.

2.5 SDS-PAGE of membrane fractions

Protein pellets from high speed ultracentrifugation were homogenized in a volume equivalent to 1/10 the initial volume of extract with 25 mM HEPES pH 7.5, containing 10 % of ethylene glycol. Protein samples were adjusted to 1 % SDS, 2.5 % β-mercaptoethanol, 10% glycerol, 0.001 % bromophenol blue and 150 mM Tris-HCl, pH 7.0, prior to separation by SDS-PAGE on a 12.5 % polyacrylamide gel in a Tris-Tricine buffer system [20]. Proteins were stained with colloidal blue G-250 as described above.

2.6 Protein digestion

Protein bands were manually excised from the gels and processed in 96-well microtitration plates using an automatic platform (EVO150, Tecan). For shotgun analysis, the protein track resulting from SDS PAGE was cut into 13 slices. Gel slices were washed in 25 mM NH_4HCO_3 for 15 min and then in 50 % (v/v) acetonitrile containing 25mM NH_4HCO_3 for 15 min. This washing procedure was repeated three times. Gel pieces were then dehydrated with 100 % acetonitrile and then incubated with 7 % H_2O_2 for 15 min before being washed again as described above. 0.15 µg of modified trypsin (Promega, sequencing grade) in 30µl of 25 mM NH_4HCO_3 was added to each gel slice for an overnight incubation at 37°C. Peptides were then extracted from gel pieces in three 15 min sequential extraction steps in 30 µL of 50% acetonitrile, 30 µL of 5% formic acid and finally 30 µL of 100% acetonitrile. The pooled supernatants were then dried under vacuum.

2.7 Nano-LC-MS/MS analysis.

For nano-LC-MS/MS analysis, the dried extracted peptides were resuspended in water containing 2.5 % acetonitrile and 2.5 % trifluoroacetic acid. A nano-LC-MS/MS analysis was then performed (Ultimate 3000, Dionex and LTQ-Orbitrap, Thermo Fischer Scientific). The system included a 300 µm x 5 mm PepMap C18 precolumn and a 75 µm x 150 mm C18 Gemini column. The column was developed at a flow rate of 300 nL/min with a 60-minute gradient from solvent A (5% acetonitrile and 0.1% formic acid in water) to solvent B (80% acetonitrile and 0.08% formic acid in water). MS and MS/MS data were acquired using Xcalibur (Thermo Fischer Scientific) and processed automatically using Mascot Daemon software (Matrix Science).

Consecutive searches against the SwissProt/TrEMBL database were performed for each sample using an intranet version of Mascot 2.0. Peptide modifications allowed during the search were N-acetylations, mono- and dioxidations (methionine), conversions to cysteic acid and methionine sulphone. Proteins showing at least two peptides with a score higher than the query threshold (p-value <0.05) were automatically validated. If one set of peptides yielded two or more proteins, and proteins were from the same organism, only the protein ranked first in the alphabetic order was validated (rejection of redundant proteins). When the proteins were from different *Mycobacterium* strains, that from *M. vanbalenii* PYR-1 was arbitrarily chosen. Proteins identified by only one peptide were checked manually using the classical fragmentation rules. The rate of false-positive protein identifications was estimated to be about 1.2% by performing a search with a SwissProt/TrEMBL decoy database according to a published procedure [4].

For each identified protein, the spectral count values were determined, and abundance rates were then calculated as percentages of the whole set of identified proteins according to the formula : Abundance of protein X = (spectral count protein X) / (Σ spectral counts for all proteins) x 100.

2.8 Cloning of the CYP153 and alkB genes

DNA fragments containing *alkB1* alone , *alkB1-rubA1-rubA2, alkB1-rubA1-rubA2-tetR,* and *alkB2* were separately PCR-amplified using appropriate primers and genomic DNA from IFP2173 prepared as previously described [8]. *CYP153* was amplified using 5'-GCATATGACCGAAATGACGGTG and 5'-CGGATCCTCAGGCGTTGATGCGCAC as forward and reverse primers, respectively. The amplicons were purified, cloned into pDRIVE (Qiagen) and sequenced on both strands. Gene sequences were validated when sequencing of replicate amplicons gave identical results. Details on the amplification and cloning procedures are available upon request. Sequence analysis was performed using BLAST.

2.9 RNA extraction and RT-PCR analysis

Total RNA was extracted from 50-mL cultures of strain IFP 2173 using standard procedures [19]. Bacteria were grown on acetate to an OD_{600} of 0.7 (control cells) or washed and resuspended to an OD_{600} of 0.6, and further incubated with 2-EHN for four days. Bacteria were then centrifuged at 10,000 × g, and resuspended in 200 µL of 20 mM Tris-HCl, 5 mM EDTA, pH 8, containing lysozyme and lysostaphin, 1.5 and 0.025 mg/mL, respectively (Sigma Life Science). After 10 min at 37°C, RNA was extracted using the RiboPure^{TM}-Bacteria kit (Ambion, Austin, Texas). Crude RNA samples (2 µg) were treated with Turbo DNase (Ambion) and the resulting RNA preparations were quantified using a Nanodrop apparatus (NanoDrop Technologies). RT-PCR was performed with 10 ng of RNA preparation using the One step RT-PCR kit (Promega, France). PCR amplification of internal gene sequences was carried out with the following primer pairs: for *alkB1*, alkB1-F (5'-CGTGATCATGGGTGCCTAC-3') and alkB1-R (5'-CCAGAACGTCTCACCGAAG-3'); for *alkB2*, alkB2-F (5'-CCTGATGTTCCTCGTGATCC-3') and alkB2-R (5'-CTTGTCGACGTCGCTCATC-3'); for CYP153, P450fw1 and P450rw3 [30]; for the aldehyde dehydrogenase encoding gene (*alkH*), ALDH1-F (5'-GCACCGTGCTGATCATCGGTGC-3') and ALDH1-R (5'-

CCAGGCGATGCGCTTGGCG-3'), for the 16S RNA gene, P16S-F (5'-GGTCTAATACCGAATACACCCTTCT-3') and P16S-R (5'-CCAGGAATTCCAGTCTCCC-3'). RT-PCR reactions were carried out as follows: 45 min at 45°C, 3 min at 95°C, then 32 cycles of 30 s at 95°C, 30 s at 62°C and 30 s at 72°C, 5 min final elongation at 72°C. Products were analyzed by electrophoresis on 2% agarose gels.

2.10 Nucleotide sequences

The nucleotide sequences of *alkB1rubA1rubA2tetR*, *alkB2*, CYP153, *alkH* (partial) were deposited under accession number FJ009005, FJ009004, FJ009003, FJ207472, respectively.

3. Results

3.1 Identification of cytoplasmic proteins up-regulated on 2-EHN

In order to identify proteins up-regulated on 2-EHN, protein profiles of cells incubated with this compound were compared to those of cells grown on acetate. Cytoplasmic proteins were prepared and analysed by 2D gel electrophoresis while membrane fractions from the high-speed centrifugation pellet of cell extracts were separated by SDS-PAGE. As discussed below, membrane fractions possibly included proteins loosely associated to membranes as well as cytoplasmic proteins trapped into membrane vesicles.

Comparison of 2D gel protein profiles revealed that 30 protein spots were either absent in acetate-grown cells or at least two-fold more abundant in 2-EHN-grown cells (Fig. 1). To confirm these results, we performed ^{35}S-labeling experiments where cells were exposed to 2-EHN for 30 h or to acetate for 6 h. This difference in incubation time was intended to reflect the much slower growth of strain IFP 2173 on 2-EHN compared to acetate. Autoradiographies of the 2D gel showed markedly different patterns (Fig. S1 in supplementary data). Most labelled proteins uniquely detected in 2-EHN-exposed cells corresponded to spots previously identified based on comparison of stained gels, but two additional 2-EHN-specific polypeptides were found (E10 and E28). The position of these extra polypeptides has been reported on the 2D image in

Fig. 1A. The 32 protein spots of interest were subjected to trypsin digestion followed by LC-MS/MS analysis and search for peptide matches in the data bases using Mascot (see Materials and Methods for details). Thanks to the high accuracy and wide dynamic range of the mass spectrometer, several spots were found to contain 2- to 4 imperfectly separated proteins. Spots E2, E3, E4, E7, E12, E18, E22 and E24 yielded two protein identifications, spots E1, E9 and E10 yielded three and spot E23 gave four. On the other hand, a few pairs of closely-located spots gave single protein identifications. As a result, the analysis of 32 spots ended up with a total of 42 proteins, which matched orthologs found in *M. vanbalenii* PYR-1 and related *Mycobacterium* strains from soil (Table 1). One set of induced proteins was clearly associated with the β-oxidation of fatty acids. Some of the enzymes involved in this pathway were found in multiple isoforms, including acetyl-CoA acyltransferase (2 copies), acyl-CoA dehydrogenase (7 copies), enoyl-CoA hydratase/isomerase (4 copies). Consistent with this finding, the reference *Mycobacterium* strains mentioned above were found to contain multiple gene copies coding for enzymes of the β-oxidation in their genome (Table S1). Other proteins up-regulated on 2-EHN included dehydrogenases, diverse metabolic enzymes and proteins involved in cell response to stress (Table 1).

3.2 2-EHN-induced proteins associated to membrane fractions

Since membrane proteins are generally difficult to analyze by regular 2D gel electrophoresis, we chose to separate the proteins of the insoluble high-speed fractions of cell extracts by one dimension SDS-PAGE. When stained protein profiles of 2-EHN versus acetate-grown cells were compared no obvious differences were observed. However, ^{35}S radioactive labelling revealed that some protein bands became clearly labelled upon exposure to 2-EHN, including a prominent 45-kDa protein (Fig. S2**)**. In order to identify proteins of interest, protein sets from 2-EHN and acetate grown cells were separated by SDS-PAGE, and subjected to trypsin-digestion and peptide

analysis by LC-MS/MS. Data processing using Mascot identified over 1300 proteins, most of which had counterparts in the proteome of *M. vanbalenii* PYR-1. Search for membrane-bound proteins using the HMMTOP software [27] revealed that about 30% of this set of proteins potentially showed at least one transmembrane segment. In addition, an unknown proportion of the detected proteins were probably membrane-associated through hydrophobic interactions or as part as membrane-bound complexes However, many proteins recovered in the membrane fraction were cytoplasmic, indicating that they might have been trapped in membrane vesicles that formed upon cell lysis.

An inventory of proteins found to be common or specific to cells incubated with 2-EHN or acetate is presented in tables S2 and S3 in supplementary material. From the set of common proteins, a subset was selected based on abundance rates more than twice as high for the 2-EHN treated cells as compared to control cells. The proteins of this subset (65 proteins) as well as those found to be specific to the 2-EHN treatment (300 proteins) were tentatively classified in terms of enzyme category or metabolic function, with special emphasis on enzymes related to alkane degradation (Table 2). A comparison of this set of proteins with that found by the 2D gel analysis revealed that only 9 proteins were common to both sets (Table 1). A total of 17 proteins were found to be enzymes of the β-oxidation of fatty acids, including many redundant isoforms, five of which were also detected on 2D gels (A1TCG6, A1TDA6, A1T5U2, A1TE56 and A1TDW4). Consistent with the 2D gel data, numerous proteins up-regulated on 2-EHN were dehydrogenases including 12 short-chain dehydrogenase/reductases (SDR). Several proteins were likely involved in the response to stress, other presumably act as transcriptional regulators.

The analysis highlighted two alcohol dehydrogenases (ADH) and one aldehyde dehydrogenase (ALDH) possibly implicated in the early steps of the 2-EHN degradation pathway (see below). Besides, enzymes of the central metabolism previously shown to be essential for alkane assimilation [18] have been detected, including two phosphoenolpyruvate synthases involved in

gluconeogenesis. Enzymes related to the metabolism of lipids were also identified, suggesting that membrane modifications might occur as part of the bacterial adaptation to growth on a hydrophobic substrate.

Four cytochromes P450 were identified, two of which belong to the CYP153 subclass of P450, potentially capable of alkane hydroxylation. The most abundant of the two enzymes, identified by 11 peptides (36% coverage), was found to be closely related to the CYP153 enzyme from *Mycobacterium* sp. XHN-1500 [31].

Membrane proteins relevant to the metabolism of alkanes were not detected in either protein extract. This is the case for the trans-membrane AlkB hydroxylase that is known to catalyze the initial oxidation reaction of alkanes in many bacteria [29].

3.3 Occurrence of several putative alkane monooxygenases in strain IFP 2173

Our proteomic analysis revealed that one cytochrome P450 with close similarity with a well characterized alkane hydroxylase (CYP153) was 2-EHN-specific. In order to learn more about this protein, its structural gene was PCR-amplified using genomic DNA from strain IFP 2173 and specific oligonucleotides designed based on the gene sequence of *CYP153A* from strain XHN-1500 [31]. A 1261 bp gene was obtained, which displayed high sequence similarity with its counterpart from strain XHN-1500 (99 % identities), resulting in a predicted protein having only two amino acid changes compared to CYP153A.

In a previous study, a gene potentially involved in isoalkane degradation was found in strain IFP 2173 and identified as an *alkB* gene based on partial sequence determination [23]. A BLAST search showed than this gene was closely related to *alkB* from *M. vanbaalenii* PYR-1. This strain has two alkane monooxygenase genes, one of which is associated with two genes encoding rubredoxins. Primers were designed after the *alkB* gene sequences of *M. vanbaalenii* PYR-1, and used to amplify corresponding genes from strain IFP 2173 genomic DNA. Two *alkB*-like genes

were found in two separate loci, which displayed exactly the same gene arrangement as that found in *M. vanbaalenii* PYR-1. In particular, the *alkB1* gene was followed by two rubredoxin genes, named *rubA1* and *rubA2*, almost identical to counterpart genes of *M. vanbaalenii* PYR-1 (99% identity). The second *alkB* gene (*alkB2*) was 98% identical to its counterpart in strain PYR-1.

3.4 RT-PCR evidence for the expression of three alkane hydroxylases in 2-EHN fed cells

Since none of the AlkB-like hydroxylases was detected in extracts of strain IFP 2173 upon proteomic analysis, we carried out RT-PCR experiments to determine whether the corresponding genes were expressed under the growth conditions used in this study. Transcripts of the *alkB1* and *alkB2* genes were equally detectable in acetate and 2-EHN-fed cells (Fig. 2). Further analysis showed that a transcript specific for the gene encoding the CYP153 hydroxylase described above was also detected in both 2-EHN and acetate-grown cells (Fig. 2). This finding is consistent with the fact that the enzyme was clearly identified by proteomic analysis in 2-EHN-fed cells but contrasted with the finding that it was not found in acetate-grown cells. Perhaps cells growing on acetate produce the CYP153 protein at a low level or in a transient manner during a particular phase of growth, so that it passed undetected.

A single ALDH appeared to be up-regulated in 2-EHN-fed cells to a level at least 2-fold as high as in acetate-grown cells. Using primers designed after the gene encoding an orthologous ALDH from strain PYR-1 (A1P1A6), a DNA fragment that perfectly matched the target gene sequence, was PCR-amplified from IFP 2173 genomic DNA. RT-PCR indicated that this gene was transcribed in both acetate and 2-EHN fed cells (Fig. 2). The deduced sequence of the closely related PYR-1 enzyme displayed 39% sequence identity with the product of the *alkH* gene from *P. putida* GPo1.

4. Discussion

The present study deals with the metabolic adaptation of a bacterium which was forced to grow on a xenobiotic compound being a poor carbon source and a toxic substance. Our proteomic analysis identified over 1300 proteins based on sequence information available in the data bases even though the genome of strain IFP 2173 was unknown. Most proteins were identified as orthologs from strain *M. vanbaalenii* PYR-1 or related *Mycobacterium* species, thus reflecting the high degree of conservation of protein sequences in the proteomes from fast-growing *Mycobacterium* species isolated from various places around the world. Besides catabolic enzymes enabling the bacterium to utilize 2-EHN as carbon source, many up-regulated proteins were found to be involved in lipid metabolism, regulation and response to stress, and might help bacteria to adapt to the toxic and/or hydrophobic character of 2-EHN. The following discussion focuses on enzymes that might be implicated in 2-EHN degradation**.**

In a previous study, we showed that strain IFP 2173 partially degraded 2-EHN to a compound identified as 4-ethyltetrahydrofuran-2(3H)-one, and we proposed a degradation pathway outlined in figure 3 [17]. Every step in the pathway can be assigned at least one enzyme found among the proteins up-regulated on 2-EHN, except for the last step of the β-oxidation which is catalyzed by a thiolase. Since three thiolase genes are present in the genomes of three related *Mycobacterium* species (Table S1), at least one thiolase is expected to be produced by strain IFP 2173 grown on 2-EHN. Perhaps, the enzyme was synthesized in small amounts and passed undetected in our proteomic analysis.

We identified four alkane hydroxylases that might catalyze the first step in 2-EHN degradation *i.e*. the hydroxylation of the distal methyl group. Two enzymes are similar to the classical AlkB membrane-bound enzymes that were found to play a pivotal role in alkane degradation by *P. putida* GPo1 [28] and A. *borkumensis* SK2 [21]. The AlkB proteins were not detected in the membrane fraction of IFP 2173 in either growth conditions, even when searching the proteomic

data for the expected peptides derived from their deduced protein sequence. Nevertheless, specific transcripts for the corresponding genes were found in cells grown on acetate or exposed to 2-EHN suggesting that the proteins were synthesized. Perhaps, the AlkB proteins were poorly solubilized in SDS or yielded few tryptic peptides detectable by LC-MS/MS. The two other plausible enzymes that can initiate 2-EHN degradation are soluble cytochromes P450 of the CYP153 subfamily. Although many genes encoding cytochromes P450 are present in the genomes of related *Mycobacterium* species (Table 2), sequence alignments indicated that none of the gene products was related to the CYP153 (data not shown). In addition, the CYP153 proteins identified in strain IFP 2173 were found to be mainly produced on 2-EHN, suggesting that at least one of these enzymes takes part in the degradation. CYP153 cytochromes hydroxylate linear or cyclic alkanes with medium chain length [31]. For instance, the CYP153A6 from *Mycobacterium* sp. XHN1500, which is the closest ortholog of the major CYP153 from IFP 2173, preferentially utilizes octane [31], but can also hydroxylate substrates with a bulky structure like limonene [31]. CYP153-like genes have been found in other Actinomycetes as well as in α and β-proteobacteria, and three groups were distinguished based on phylogenetic considerations [29]. Like other bacterial cytochromes, the CYP153 enzymes function with two electron carriers, a NAD(P)H-oxidoreductase and a ferredoxin. In this respect, a FAD-binding oxidoreductase that might be functionally associated with one of the CYP153 from IFP 2173 has been identified by the 2D gel approach (Table 1), and four such reductases were detected by the shotgun approach (Tables S2 & S3).

An esterase is also required to hydrolyze the nitro-ester bond of 2-EHN. A chloride peroxidase was found among the 2-EHN-induced proteins in the 2D gel analysis (A1T5E7), which showed the classical consensus sequence (G*X*S*X*G) typical for the active site of esterases. This type of enzyme is active on carboxylic esters [2], but it is unknown whether it could remove the nitro group of 2-EHN. Four other putative esterases up-regulated on 2-EHN can potentially catalyze

this reaction (Tables S2 & S3). Since strain IFP 2173 can use 2-ethylhexanol and transform it to 2-ethylhexanoic acid and 4-ethyltetrahydrofuran-2(3H)-one [17], it may be inferred that hydrolysis of the ester bond precedes the hydroxylation of the distal methyl group in the biodegradation pathway.

The subsequent step in the degradation pathway is the conversion of the 2-ethylpentane-1,5-diol to an aldehyde by an ADH. Three 38-kDa ADH were apparently associated to 2-EHN metabolism, which are predicted to have a zinc-binding domain and a GroES-like structure. A different and larger ADH (AlkJ; 61 kDa) is involved in alkane oxidation in *P. putida* GPo1. However, a deletion of *alkJ* did not affect alkane degradation, indicating that this reaction does not require a specific ADH [28].

A single 2-EHN-specific ALDH was detected by SDS-PAGE and peptide analysis. Examination of the sequence of the orthologous enzyme of strain PYR-1 (A1T1A6) showed that it might be composed of a catalytic domain and a LuxC-like domain [15]. The detected ALDH showed 39 % sequence identity with AlkH encoded by the *alk* operon, which is involved in alkane biodegradation in *P. putida* GPo1 [32].

The biosynthesis of multiple isoenzymes of the β-oxidation pathway in response to cell exposure to 2-EHN is intriguing. Many *Mycobacterium* species are known to thrive on alkanes, but the redundancy of β-oxidation enzymes had not been previously reported, although it could be predicted from the abundance of genes coding for such enzymes in available genome sequences of *Mycobacteria* (Table S1). In contrast, the hydrocarbonoclastic bacterium *A. borkumensis* SK2 produced relatively few specific enzymes when growing on alkanes [18]. Perhaps, the greater number of isoenzymes found in soil *Mycobacteria* reflects a more versatile metabolism, adapted to a diet made of diverse hydrocarbons present in their environment.

In our study, we identified most of the enzymes possibly involved in 2-EHN degradation by strain IFP 2173. Since these enzymes have counterparts in other soil *Mycobacteria*, the question

arises whether these bacteria can degrade 2-EHN. We recently found that this ability is in fact restricted to a few *M. austroafricanum* strains [21]. Hence, 2-EHN degradation might depend on the catalytic activity of some specific enzyme such as a CYP153 hydroxylase, which is present in strain IFP 2173 but absent in related *Mycobacteria* including strain PYR-1. Accordingly, we observed that strain PYR-1 cannot utilize 2-EHN as carbon source (unpublished results).

Acknowledgements

This work was supported by grants from the Centre National de la Recherche Scientifique, the Commissariat à l'Energie Atomique and University J. Fourier to UMR5249. E. Nicolau thanks the Association Nationale de la Recherche Technique for a doctoral fellowship. We thank C. Meyer and M. Louwagie for technical assistance and J. C. Willison for critical reading of the manuscript.

References

1 Ban-Weiss, G.A., Chen, J.Y., Buchholz, B.A., and Dibble, R.W. (2007). A numerical investigation into the anomalous slight NOx increase when burning biodiesel; A new (old) theory. Fuel Process. Technol. 88, 659-667.

2 Bornscheuer, U.T. (2002). Microbial carboxyl esterases: classification, properties and application in biocatalysis. FEMS Microbiol. Rev. 26, 73-81.

3 Dean-Ross, D., and Cerniglia, C.E. (1996). Degradation of pyrene by *Mycobacterium flavescens*. Appl Microbiol. Biotechnol. 46, 307-312.

4 Elias, J.E., and Gygi, S.P. (2007). Target-decoy search strategy for increased confidence in large-scale protein identifications by mass spectrometry. Nature Methods 4, 207-214.

5 Francois, A., Mathis, H., Godefroy, D., Piveteau, P., Fayolle, F., and Monot, F. (2002). Biodegradation of methyl tert-butyl ether and other fuel oxygenates by a new strain, *Mycobacterium austroafricanum* IFP 2012. Appl. Environ. Microbiol. 68, 2754-2762.

6 Gallien, S., Perrodou, E., Carapito, C., Deshayes, C., Reyrat, J.M., Van Dorsselaer, A., Poch, O., Schaeffer, C., and Lecompte, O. (2009). Ortho-proteogenomics: multiple proteomes investigation through orthology and a new MS-based protocol. Genome Res. 19, 128-135.

7 Gołofit-Szymczak, M. (2005). 2-EHN Documentation. In: International Journal Of Occupatioinal Safety dand Ergonomics, CIOP PIP, Warszawa, Czerniakowska.

8 Heiss-Blanquet, S., Benoit, Y., Marechaux, C., and Monot, F. (2005). Assessing the role of alkane hydroxylase genotypes in environmental samples by competitive PCR. J Appl .Microbiol. 99, 1392-1403.

9 Kim, S.J., Kweon, O., and Cerniglia, C.E. (2009). Proteomic applications to elucidate bacterial aromatic hydrocarbon metabolic pathways. Curr. Opin. Microbiol. 12, 301-309.

10 Krivobok, S., Kuony, S., Meyer, C., Louwagie, M., Willison, J.C., and Jouanneau, Y. (2003). Identification of pyrene-induced proteins in *Mycobacterium* sp. strain 6PY1: evidence for two ring-hydroxylating dioxygenases. J. Bacteriol. 185, 3828-3841.

11 Laemmli, U.K. (1970). Cleavage of structural proteins during the assembly of the head of bacteriophage T4. Nature 227, 680-685.

12 Lee, M., Kim, M.K., Kwon, M.J., Park, B.D., Kim, M.H., Goodfellow, M., and Lee, S.T. (2005). Effect of the synthesized mycolic acid on the biodegradation of diesel oil by *Gordonia nitida* strain LE31. J. Biosci. Bioeng. 100, 429-436.

13 Lopes Ferreira, N., Maciel, H., Mathis, H., Monot, F., Fayolle-Guichard, F., and Greer, C.W. (2006). Isolation and characterization of a new *Mycobacterium austroafricanum* strain, IFP 2015, growing on MTBE. Appl. Microbiol. Biotechnol. 70, 358-365.

14 Maier, T., Forster, H.H., Asperger, O., and Hahn, U. (2001). Molecular characterization of the 56-kDa CYP153 from *Acinetobacter* sp. EB104. Biochem. Biophys. Res. Commun. 286, 652-658.

15 Marchler-Bauer, A., Anderson, J.B., Derbyshire, M.K., DeWeese-Scott, C., Gonzales, N.R., Gwadz, M., Hao, L., He, S., Hurwitz, D.I., Jackson, J.D.*, et al.* (2007). CDD: a conserved domain database for interactive domain family analysis. Nucleic Acids Res. 35, D237-240.

16 Neuhoff, V., Arold, N., Taube, D., and Ehrhardt, W. (1988). Improved staining of proteins in polyacrylamide gels including isoelectric focusing gels with clear background at nanogram sensitivity using Coomassie Brilliant Blue G-250 and R-250. Electrophoresis 9, 255-262.

17 Nicolau, E., Kerhoas, L., Lettere, M., Jouanneau, Y., and Marchal, R. (2008). Biodegradation of 2-ethylhexyl nitrate by *Mycobacterium austroafricanum* IFP 2173. Appl. Environ. Microbiol. 74, 6187-6193.

18 Sabirova, J.S., Ferrer, M., Regenhardt, D., Timmis, K.N., and Golyshin, P.N. (2006). Proteomic insights into metabolic adaptations in *Alcanivorax borkumensis* induced by alkane utilization. J. Bacteriol. 188, 3763-3773.

19 Sambrook, J., Fritsch, E.F., and Maniatis, T., eds. (1989). Molecular Cloning: a laboratory manual. Second edition. Cold Spring Harbor Laboratory Press, Cold Spring Harbor, NY.

20 Schagger, H. (2006). Tricine-SDS-PAGE. Nat. Protoc. 1, 16-22.

21 Schneiker, S., Dos Santos, V.A., Bartels, D., Bekel, T., Brecht, M., Buhrmester, J., Chernikova, T.N., Denaro, R., Ferrer, M., Gertler, C*., et al.* (2006). Genome sequence of the ubiquitous hydrocarbon-degrading marine bacterium *Alcanivorax borkumensis*. Nat. Biotechnol. 24, 997-1004.

22 Sokolovska, I., Rozenberg, R., Riez, C., Rouxhet, P.G., Agathos, S.N., and Wattiau, P. (2003). Carbon source-induced modifications in the mycolic acid content and cell wall permeability of *Rhodococcus erythropolis* E1. Appl. Environ. Microbiol. 69, 7019-7027.

23 Solano-Serena, F., Marchal, R., Heiss, S., and Vandecasteele, J.P. (2004). Degradation of isooctane by *Mycobacterium austroafricanum* IFP 2173: growth and catabolic pathway. J. Appl. Microbiol. 97, 629-639.

24 Solano-Serena, F., Nicolau, E., Favreau, G., Jouanneau, Y., and Marchal, R. (2008). Biodegradability of 2-ethylhexyl nitrate (2-EHN), a cetane improver of diesel oil. Biodegradation 20, 85-94.

25 Szybist, J.P., Boehman, A.L., Taylor, J.D., and McCormick, R.L. (2005). Evaluation of formulation strategies to eliminate the biodiesel NOx effect. Fuel Proces. Technol. 86, 1109-1126.

26 The American Chemistry Council Petroleum additives panel (2006). High Production Volume Challenge program Final Submission for Nitric Acid, 2-Ethylhexyl Ester, pp. 11.

27 Tusnady, G.E., and Simon, I. (2001). The HMMTOP transmembrane topology prediction server. Bioinformatics 17, 849-850.

28 van Beilen, J.B., Eggink, G., Enequist, H., Bos, R., and Witholt, B. (1992). DNA sequence determination and functional characterization of the OCT-plasmid-encoded alkJKL genes of *Pseudomonas oleovorans*. Mol. Microbiol. 6, 3121-3136.

29 van Beilen, J.B., and Funhoff, E.G. (2007). Alkane hydroxylases involved in microbial alkane degradation. Appl. Microbiol. Biotechnol. 74, 13-21.

30 van Beilen, J.B., Funhoff, E.G., van Loon, A., Just, A., Kaysser, L., Bouza, M., Holtackers, R., Rothlisberger, M., Li, Z., and Witholt, B. (2006). Cytochrome P450 alkane hydroxylases of the CYP153 family are common in alkane-degrading eubacteria lacking integral membrane alkane hydroxylases. Appl. Environ. Microbiol. 72, 59-65.

31 van Beilen, J.B., Holtackers, R., Luscher, D., Bauer, U., Witholt, B., and Duetz, W.A. (2005). Biocatalytic production of perillyl alcohol from limonene by using a novel *Mycobacterium* sp. cytochrome P450 alkane hydroxylase expressed in *Pseudomonas putida*. Appl. Environ. Microbiol. 71, 1737-1744.

32 van Beilen, J.B., Panke, S., Lucchini, S., Franchini, A.G., Rothlisberger, M., and Witholt, B. (2001). Analysis of *Pseudomonas putida* alkane-degradation gene clusters and flanking insertion sequences: evolution and regulation of the alk genes. Microbiology 147, 1621-1630.

33 Wang, R.F., Cao, W.W., and Cerniglia, C.E. (1995). Phylogenetic analysis of polycyclic aromatic hydrocarbon degrading mycobacteria by 16S rRNA sequencing. FEMS Microbiol. Lett. 130, 75-80.

34 Zhao, B., and Poh, C.L. (2008). Insights into environmental bioremediation by microorganisms through functional genomics and proteomics. Proteomics 8, 874-881.

Legends to figures

Figure 1: 2D gel map of soluble proteins from *M. austroafricanum* IFP 2173 induced by 2-EHN. Isoelectric focusing was performed in the pH range 4 to 7. **A**: cells grown on 2-EHN, **B**: cells grown on acetate. 2-EHN-specific protein spots are numbered in panel A.

Figure 2 : Expression of genes relevant to 2-EHN degradation as analyzed by RT-PCR. Reactions were performed as described under Materials and Methods using primers specific to an internal region of the indicated genes. *alkB1* and *alkB2* designate genes encoding two alkane hydroxylases, while *alkH* refers to a gene coding for an aldehyde dehydrogenase (see text). RNA used as template was extracted either from 2-EHN exposed cells (lanes 3 & 4) or from acetate-grown cells (lanes 5 & 6). The content of each RNA preparation was checked by carrying out a RT-PCR of a portion of 16S RNA. Lanes 3 and 5 are control reactions in which reverse transcriptase was omitted. Lane 1, DNA ladder ; lane 2, PCR amplicon generated from gDNA.

Figure 3 : Proposed pathway and enzymes involved in 2-EHN degradation

Products: **a**: 2-ethylhexyl nitrate; **b**: 2-ethylpentane-1,5-diol; **c**: 5-(hydroxymethyl)heptanoic acid; **d**: 5-(hydroxymethyl)heptanoyl CoA; **e**: 5-(hydroxymethyl)heptan-2-enoyl CoA; **f**: 3-hydroxy-5-(hydroxymethyl)heptanoyl CoA; **g**: 5-(hydroxymethyl)-3-ketoheptanoyl CoA; **h**: 3-(hydroxymethyl)-pentanoyl CoA; **i**: 3-(hydroxymethyl)-pentanoic acid; **j**: 4-ethyldihydrofuran-2-(3H)one

Enzymes: **1**: alkane hydroxylase (AlkB1, AlkB2 or CYP153) and esterase, **2**: alcohol dehydrogenase and aldehyde dehydrogenases, **3** and **8**: acyl CoA acyltransferase, **4**: Acyl CoA dehydrogenase, **5**: Enoyl CoA hydratase, **6**: Hydroxyacyl CoA dehydrogenase, **7**: Thiolase, **9**: spontaneous cyclisation. ✦ Indicates that β-oxidation is blocked by the ethyl chain in β position.

1

Table 1: Cytoplasmic proteins up-regulated upon incubation of *M. austroafricanum* IFP 2173 on 2-EHN

Enzyme or protein function	Spot #	2-EHN induction*	^{35}S-labelling on 2-EHN*	pI[b]	Mol Mass[b]	Score	Coverage (%)	Peptides	SwissProt/ TrEMBL	Micro-organism
Fatty acid metabolism										
Acyl-CoA dehydrogenase domain protein	E1	+++	+++	5,3	41116	186	10	3	A4TFJ1	*M. gilvum* PYR-GC
	E2	+++	+++	5,4		180	9	3		
	E1	+++	+++	5,3	40821	133	11	3	A3Q1G5	*Mycobacterium* sp. JLS
	E2	+++	+++	5,4	40989	702	32	10	A1TCG6[c]	*M.vanbaalenii* PYR-1
	E3	+++	+++	5,15	42234	112	10	2	A4T8F2	*M. gilvum* PYR-GC
	E4	+++	+++	4,8	39744	265	18	4	A1TDA6[c]	*M. vanbaalenii* PYR-1
	E7	++	++	5,87	42108	118	6	2	A4TFI8	*M. gilvum* PYR-GC
	E8	+++	+	5,2	41520	585	36	9	A1T5U2[c]	*M. vanbaalenii* PYR-1
Enoyl-CoA hydratase/isomerase	E9	+++	+++	4,9	29971	133	9	2	A1TDW3	*M. vanbaalenii* PYR-1
	E10	-	+++	5,1	27387	121	11	2	A4TFL1	*M. gilvum* PYR-GC
	E9	+++	+++	4,85	27478	280	22	5	A1TE56[c]	*M. vanbaalenii* PYR-1
	E9	+++	+++	4,85	26666	35	5	1	A4TDN8	*M. gilvum* PYR-GC
3-hydroxyacyl-CoA dehydrogenase, NAD-binding	E11	++	++	5,4	76177	586	19	11	A1TF87	*M. vanbaalenii* PYR-1
	E12	++	++	5,4		381	11	7		
Acetyl-CoA C-acyltransferase (EC 2.3.1.16)	E1	+++	+++	5,4	39836	591	32	9	A1TDW4[c]	*M. vanbaalenii* PYR-1
	E13	++	+++	4,9	42130	189	11	3	A1TF88	*M. vanbaalenii* PYR-1
Acyl-ACP thioesterase	E10	-	+++	5,3	31192	117	8	2	A1T388	*M. vanbaalenii* PYR-1

Enzyme or protein function	Spot #	2-EHN induction*	^{35}S-labelling on 2-EHN*	pI[b]	Mol Mass[b]	Score	Coverage (%)	Peptides	SwissProt/ TrEMBL	Micro-organism
FAD-dependent pyridine nucleotide-disulphide oxidoreductase	E15	+++	+++	5,55	42755	319	18	5	A4TFL9	*M. gilvum* PYR-GC
	E7	+++	+	5,8		152	9	3		
Short-chain dehydrogenase/reductase	E17	+++	++	4,9	29920	164	15	3	A1T1A7[c]	*M. vanbaalenii* PYR-1
	E18	+++	+++	4,9	30143	102	10	2	Q1BFX1	*Mycobacterium* sp. MCS
(S)-2-hydroxy-acid oxidase	E30	+++	-	7	42022	169	10	3	A1T4N1	*M. vanbaalenii* PYR-1
Dihydrolipoamide dehydrogenase	E22	++	++	5,6	49719	370	18	6	A1T382	*M. vanbaalenii* PYR-1
Lysine biosynthesis										
Dihydrodipicolinate synthase	E24	++	-	5,4	31436.7	163	12	3	A1T7Q1	*M. vanbaalenii* PYR-1
Dihydrodipicolinate reductase (EC 1.3.1.26)	E23	++	-	4,8	25816	59	8	1	A1T7N8	*M. vanbaalenii* PYR-1
Protein synthesis										
Serine-tRNA ligase (EC 6.1.1.11)	E25	+++	+++	4,8	60542.4	128	6	2	A1TGX4	*M. vanbaalenii* PYR-1
Ketol-acid reductoisomerase (EC 1.1.1.86)	E3	+++	+++	5,2	36513	158	5	2	Q1BAR7	*Mycobacterium* sp. MCS
Nitrogen assimilation										
Alanine dehydrogenase (EC 1.4.1.1)	E28	-	+++	5,2	38907	203	11	3	A1T7L9	*M. vanbaalenii* PYR-1
Oxidative phosphorylation										
ATP synthase epsilon chain (EC 3.6.3.14) (ATP synthase F1 sector epsilon subunit)	E29	+++	+++	4,8	13330	85	9	1	P45822	*M. leprae* TN
CO_2 hydratation										
Carbonic anhydrase	E31	++	++	4,8	18225	272	33	6	A1TDF0	*M. vanbaalenii* PYR-1
Glycolysis / glyconeogenesis										
Phosphoglycerate kinase (EC 2.7.2.3)	E32	+++	+++	4,7	42102	435	24	6	A1T8L1	*M. vanbaalenii* PYR-1
	E6	+++	+++	4,75		572	28	8		

Enzyme or protein function	Spot #	2-EHN induction*	^{35}S-labelling on 2-EHN*	pI[b]	Mol Mass[b]	Score	Coverage (%)	Peptides	SwissProt/ TrEMBL	Micro-organism
Stress response										
Heat shock protein Hsp20	E26	+++	+++	4,8	15648.4	177	27	3	A1T4V8[c]	*M. vanbaalenii* PYR-1
UspA	E24	++	-	5,4	31354	85	5	1	A1T4W2	*M. vanbaalenii* PYR-1
Miscellaneous										
Putative esterase precursor	E18	+++	+++	5	35010	79	6	1	A1T6C2	*M. vanbaalenii* PYR-1
Chloride peroxidase (EC 1.11.1.10)	E19	++	-	5,7	30410	173	15	3	A1T5E7	*M. vanbaalenii* PYR-1
Antibiotic biosynthesis monooxygenase	E16	+++	+++	4,8	11741	56	16	1	Q1B2M9	*Mycobacterium* sp. MCS
Allophanate hydrolase subunit 1	E10	+++	+++	5,3	25092	142	10	2	A1T1V3	*M. vanbaalenii* PYR-1
Fumarate lyase	E20	+++	++	5,1	49944	579	24	10	A1TE24[c]	*M. vanbaalenii* PYR-1
	E21	+++	++	5,1	49944	538	27	8		
HpcH/HpaI aldolase	E23	++	-	4,8	29032	202	13	4	A1TCG4	*M. vanbaalenii* PYR-1
Ribonuclease PH (EC 2.7.7.56)	E23	++	-	4,8	27449	75	5	2	A1T7Q1	*M. vanbaalenii* PYR-1
Glycyl-tRNA synthetase, alpha2 dimer	E22	++	++	5,6	59543	405	18	7	A1TBP9	*M. vanbaalenii* PYR-1
3-hydroxyisobutyrate dehydrogenase precursor	E23	++	-	4,8	29262	195	16	3	A1T4U4	*M. vanbaalenii* PYR-1
Cyclic nucleotide-binding:regulatory protein, Crp	E27	+++	-	9,6	24776	409	40	7	A1T6A5	*M. vanbaalenii* PYR-1
Phosphoribosyltransferase: Erythromycin esterase	E12	++	++	5,4	74587	49	2	1	A1T4X7[c]	*M. vanbaalenii* PYR-1

*Spot intensity was estimated from visual inspection of stained gels or autoradiographies : +, ++, +++ stand for small, medium size and large spots, respectively. (-) means undetected spot.

[b] Theoretical values calculated on the basis of deduced polypeptide sequences.

[c] These protein entries also appear in the list of 2-EHN-induced proteins identified by shotgun analysis (Table S3)

Table 2: Functional classification of proteins more abundant or exclusively dete

EHN

	Number of proteins	
	exclusively found on 2-EHN	More abundant
Beta oxidation	17	1
P450 hydroxylases	4	0
Esterases	3	1
Dehydrogenases	2 ADH	1 ALI
SDR	10	2
Stress response	12	9
Regulation	21	3
Lipid metabolism/cell wall	13/1	1/3
Ribosomal proteins	12	2
N-metabolism	3	1
General metabolism	74	22
ABC transporter proteins	22	3
Other	64	6
Putative uncharacterized	42	10

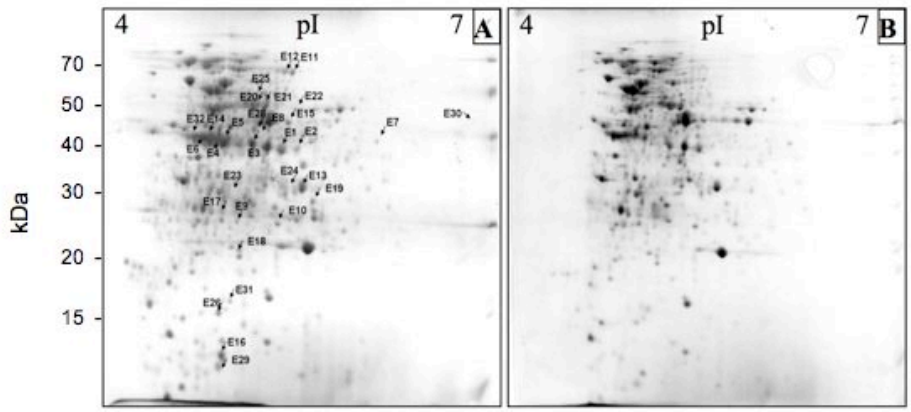

Fig. 1, Nicolau et al.

Fig. 2, Nicolau et al.

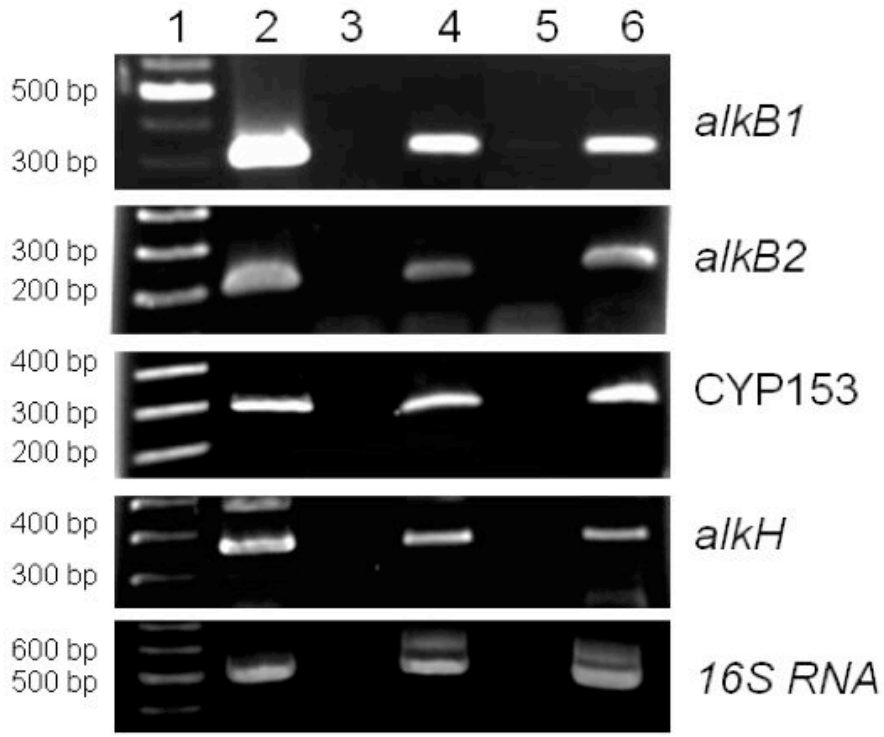

Fig. 3, Nicolau et al.